

# DISSIPATION IN RANDOM WAVE GROUPS INCIDENT ON A BEACH

by J.A. Roelvink

DELFT HYDRAULICS  
p.o. box 152  
8300 AD Emmeloord  
The Netherlands

February 13, 1992

## 1. Introduction

The transformation of certain parameters of an incident random wave train across the surf zone has been the subject of much study and modelling effort. In recent literature, two classes of models have been developed, which are both based on the wave energy balance or the wave action equation, but use markedly different approaches.

In the first, *parametric*, class of models (Battjes and Janssen, 1978; Thornton and Guza, 1983), a shape of the breaking wave height distribution is assumed, with parameters that are a function of local, time-averaged wave parameters. The dissipation per breaking wave is modelled using the analogy between fully breaking waves and bores, which was first pointed out by Le Mehaute (1962). By combination of the breaking wave height distribution and the dissipation function, the average dissipation as a function of local wave parameters is obtained. By solving the wave energy balance equation, these local wave parameters can be computed over an arbitrary profile, given the conditions at a seaward boundary.

The second, *probabilistic*, class of models takes the probability density function of wave height (and sometimes wave period) at a seaward boundary, schematizes it to a discrete number of wave height (period) classes, and assumes that each class behaves like a periodic sub-group that propagates independently of the others. (Mizuguchi, 1982; Mase and Iwagaki, 1982; Dally et al, 1984). The wave energy balance equation is then solved separately for all waves. As a result, at each point along the profile, the wave height distribution can be determined. All models in this class separate the description for each wave into its behaviour before and after its breakpoint.

Both classes of models, when calibrated, may serve well to predict the transformation of certain properties of the wave height distribution across the surf zone. Also, wave-averaged parameters such as radiation stress and mass flux, required for the prediction of the mean set-up and the undertow are predicted satisfactorily by both classes of models.

Recently, there has been a growing recognition of the importance of variations in short-wave properties on the time-scale of wave groups. Such variations can force long-wave motions that may be important in themselves or through their interaction with wave groups (Symonds et al, 1982; Symonds and Bowen, 1984; List, 1990; Schaeffer et al, 1990). A new class of *dynamic* models (Sato, 1991; Roelvink, 1991; Symonds and Black, 1991) takes into account variations on this time-scale. The dissipation of the short-wave motion in this class of models is slowly-varying on the time-scale of the wave groups. Although the propagation and decay of wave groups, and hence the excited long-wave motions, often depend critically on the formulation of this dissipation term, a satisfactory formulation has not yet been presented.

The main goal of this study is to develop a suitable formulation for the time-varying dissipation due to wave breaking. As it is impossible to measure the time-varying dissipation directly, the formulation can only be checked by building it into models that predict measurable parameters, such as the average dissipation, the fraction of breaking waves and the mean wave energy, and by verifying these models both externally and internally.

For this purpose, one wave propagation model of the probabilistic class and three models of the parametric class were formulated, calibrated and verified in this study, all based on the same dissipation formulation. Although it has not been the primary goal of the study, these models are an interesting by-product in themselves.

The main product, however, is a calibrated formulation for the dissipation of short-wave energy as a function of energy and water depth, which can be easily implemented in models that are time-dependent on the wave-group scale.

## **2. Dissipation model**

### **Basic concept**

In a random wave train, the process of energy dissipation due to wave breaking is extremely complex. If it were possible to plot a time series of the instantaneous dissipation rate at a given location, this would show

intermittent peaks with random height and spacing, which cannot be described in a deterministic way. Even when a moving average is applied over some short-wave periods, the slowly-varying dissipation rate will still have a random component. However, we can expect this slowly-varying dissipation rate to also have a systematic component which depends on slowly-varying characteristics of the short waves, in particular the wave energy. This systematic component, which is the expected value of the dissipation rate per unit area,  $D$ , can itself be seen as the product of two components:

$$D = P_b D_b \quad [1]$$

where  $P_b$  is the probability that a wave is breaking and  $D_b$  the expected value of the dissipation rate in a breaking wave, given that its energy density is  $E$ . Both  $P_b$  and  $D_b$  vary on the time-scale of the wave groups.

### Dissipation in a breaking wave

In order to model the dissipation  $D_b$  in a breaking wave, we use the well-known analogy between breaking waves and bores, which results in the following approximate expression (Battjes & Janssen, 1978):

$$D_b = \frac{\alpha}{4} \rho g f \frac{H^3}{h} \quad [2]$$

where  $f$  is the frequency,  $H$  is the height of the breaking wave,  $h$  the water depth and  $\alpha$  a calibration coefficient. Battjes & Janssen assume all breaking waves to have the maximum wave height  $H_m$ ; as this maximum wave height is of the order of the water depth, the expression reduces to:

$$D_b = \frac{\alpha}{4} \rho g f H_m^2 \quad [3]$$

As in our case the height of breaking waves is allowed to be considerably smaller than the maximum wave height, expression [2] should be used in principle. However, it can be argued (Stive & Dingemans, 1984), that the water depth in equation [2] should rather be seen as a 'penetration depth', which is of the order of the wave height. In this case, the dissipation can be written as a simple function of the energy of the breaking waves:

$$D_b = 2 \alpha f_p E \quad [4]$$

where the peak frequency  $f_p$  has been taken as a characteristic measure of the frequency.

## Probability of breaking

In general, waves break when locally the wave front becomes too steep. For irregular waves this may be the result of several mechanisms, such as interaction between short waves, interaction between wave and bottom or between wave and current or wind. For simplicity, we shall not consider the effects of current or wind on wave breaking. Even then, the processes involved are extremely complex and no accurate model is available to predict the probability of breaking in irregular waves. Therefore, a simple empirical approach is chosen, based on some crude assumptions.

These assumptions are:

1. The probability of breaking depends only on local and instantaneous wave parameters. In reality, it also depends on the history of the individual waves, but the breaking process, especially in random waves, has a time-scale which is short compared to the wave group scale, so this effect can be neglected.
2. The basic parameters governing the probability of breaking are the local and instantaneous wave energy and the water depth.
3. In principle, waves of any energy may be breaking or non-breaking. However, the probability of breaking should increase monotonically towards 1 for increasing energy or decreasing water depth.

Thornton and Guza (1983) propose the following empirical 'weighting function', which can be interpreted as the probability of breaking:

$$P_b = \left[ \frac{H_{rms}}{\gamma h} \right]^n \left[ 1 - \exp \left[ - \left[ \frac{H}{\gamma h} \right]^2 \right] \right] \leq 1 \quad [5]$$

According to this expression, the probability that a particular wave in an irregular wave train is breaking not only depends on the height of this wave relative to the water depth, but also on a characteristic height parameter of the whole wave train (i.e.  $H_{rms}$ ). This would imply that the breaking process in a given wave group is influenced by events on a much greater time-scale, which seems unlikely and is in contradiction with our assumption 1. We therefore propose a different form:

$$P_b(E, h) = 1 - \exp \left[ - \left( \frac{E}{\gamma^2 E_{ref}} \right)^{n/2} \right] \quad [6]$$

with:  $E_{ref} = \frac{1}{8} \rho g h^2$

where  $\gamma$  and  $n$  are coefficients. In Figure 1 this function is plotted for several values of  $n$ . It can be seen that the steepness of the function increases with increasing  $n$ . The two coefficients  $\gamma$  and  $n$  will have to be determined empirically.

#### **Conditional expected dissipation rate for waves with given energy**

The expected dissipation rate, given a specific value of  $E$ , is now simply found by substituting equations [4] and [6] into equation [1], which leads to:

$$D = \left[ 1 - \exp \left[ - \left( \frac{E}{\gamma^2 E_{ref}} \right)^{n/2} \right] \right] * 2 \alpha f_p E \quad [7]$$

This equation describes the dissipation rate for a given (random) wave energy and water depth, as is the the main goal of this study. The calibration of the coefficients  $\alpha$ ,  $\gamma$  and  $n$  and the verification of the formulation as such is described in the following Sections.

### 3 Transformation of wave energy distribution

#### 3.1 Probabilistic model

The formulation for the *probabilistic* approach can be derived readily from the wave action equation by assuming that the slowly-varying cross-shore velocity is small compared to the group velocity  $C_g$ . This is a reasonable assumption, except for a limited area near the swash zone, where the group velocity goes to zero and the long-wave velocities increase.

Under this assumption, the wave action equation reduces to the wave energy balance:

$$\frac{\partial E}{\partial t} + \frac{\partial}{\partial x}(E C_g) = -D \quad [8]$$

Assuming  $C_g$  to be constant in time, the rate of change of the energy flux of a (part of a) wave group as it travels towards the shore is described by:

$$\frac{d}{dx}(E C_g) = -D \quad [9]$$

The dissipation rate  $D$  depends on local wave parameters and the slowly-varying water depth. Except, again, for the swash zone, the slow fluctuations in the water level can be neglected. In this case, the time-dependence vanishes from the equation, so it can be solved for any given (seaward) boundary value of  $E$ . In other words, we can follow any part of a wave group through the surf zone using this equation. As a result, we can also compute the transformation of the energy distribution through the surf zone, starting from a given distribution of  $E$  in deep water.

In deep water, it is reasonable to assume a Rayleigh-distribution for the wave height; this is equivalent to an exponential distribution for the wave energy:

$$P(\underline{E} < E) = 1 - \exp\left(-\frac{E}{\bar{E}}\right) \quad [10]$$

where  $\bar{E}$  is the time-averaged wave energy and  $P$  is the probability of non-exceedance.

In order to compute the transformation of this distribution, the distribution at deep water is given as a number of energy levels with decreasing probability of exceedance. For each deep water energy level, equation [9] is solved by explicit numerical integration. The result is a number of wave

energy decay lines, which cannot cross each other. This is due to the assumptions made in this model, namely a constant group velocity and a dissipation model which is monotonically dependent on the local wave energy.

As a result, a line which starts at an energy level with a certain probability of exceedance will represent this probability throughout the surf zone. At any computation point along the profile, the distribution of the wave energy can be reassembled from these lines. The mean wave energy can be computed from this distribution. Also, the total fraction of breaking waves can be deduced from the model.

The distribution of wave energy can be used to predict the wave height distribution by means of a suitable non-linear local wave model, which uses energy, peak frequency and water depth as input. Here, we apply the high-order stream function method as described by Rienecker & Fenton (1981). Results are presented below.

### 3.2 Parametric models

#### Basic concept

In the *parametric* class of models, the energy balance equation [8] is averaged over a time scale which is large compared with the wave group time scale:

$$\overline{\frac{\partial E}{\partial t}} + \overline{\frac{\partial}{\partial x}(E C_g)} = -\overline{D} \quad [11]$$

Assuming a stationary wave field and no correlation between wave energy and group velocity, this equation reduces to:

$$\frac{\partial}{\partial x}(\overline{E} \overline{C}_g) = -\overline{D} \quad [12]$$

The mean dissipation can be described as the weighted average of the dissipation function:

$$\overline{D} = \int_0^{\infty} p(E) D(E) dE \quad [13]$$

where  $p(E)$  is the local probability density function (pdf) of the wave energy. In order to close the equations, an assumption must be made regarding the shape of this function, depending on the local wave parameters. The scaling of the function then follows from the requirements that the function is a pdf:

$$\int_0^{\infty} p(E) dE = 1 \quad [14]$$

and that the first moment equals the mean energy:

$$\int_0^{\infty} p(E) E dE = \overline{E} \quad [15]$$

In the following, three parametric probability density functions are discussed, viz. a depth-limited Weibull-distribution, the Rayleigh-distribution and the clipped Rayleigh-distribution according to Battjes and Janssen (1978).

The following parameters will be used in order to simplify the equations:

$$E_{ref} = \frac{1}{8} \rho g h^2, \quad \sigma = \sqrt{\frac{\overline{E}}{E_{ref}}}, \quad E_* = \frac{E}{\overline{E}}, \quad Q_b = \int_0^{\infty} P_b(E) p(E) dE$$

## Weibull distribution

Klopman and Stive (1989) propose a wave height distribution, based upon a shape originally proposed by Glukhovskiy (1966), which degenerates to a Rayleigh-distribution in deep water, but has a depth-limitation resulting in a gradual deformation of the distribution for decreasing water depth. In terms of wave energy, this distribution can be written as:

$$P(\underline{E} < E) = 1 - \exp \left\{ -A \left( \frac{E}{\bar{E}} \right)^m \right\} \quad [16]$$

Here,  $m$  is a free parameter for which Klopman and Stive propose a formulation, which is rewritten here in terms of energy:

$$m = 1 + 0.7 \tan^2 \left( \frac{\pi}{2} \frac{1}{\gamma_2} \sqrt{\frac{E}{\bar{E}_{ref}}} \right) = 1 + 0.7 \tan^2 \left( \frac{\pi}{2} \frac{\sigma}{\gamma_2} \right) \quad [17]$$

The value of  $\gamma_2$  as given by Klopman and Stive is the theoretical maximum of the wave height over depth ratio, 0.833. The maximum value for the energy-related  $\sigma$ -value as defined above is in the order of 30 % lower, due to the non-linearity of depth-limited waves. Therefore a value of 0.65 has been used here.

The parameter  $A$  is linked to  $m$  through the requirement given by equation [15]:

$$A = \left[ \Gamma \left( 1 + \frac{1}{m} \right) \right]^m \quad [18]$$

The probability density function is found by differentiating equation [16]:

$$p(E) = \frac{m A}{\bar{E}} \left( \frac{E}{\bar{E}} \right)^{m-1} \exp \left\{ -A \left( \frac{E}{\bar{E}} \right)^m \right\} \quad [19]$$

The mean dissipation is now found by integration of equation [13]:

$$\begin{aligned} \bar{D} &= \int_0^{\infty} p(E) P_b(E) D_b(E) dE = \\ &= \int_0^{\infty} \frac{m A}{\bar{E}} \left( \frac{E}{\bar{E}} \right)^{m-1} \exp \left\{ -A \left( \frac{E}{\bar{E}} \right)^m \right\} \left[ 1 - \exp \left[ - \left( \frac{E}{\gamma^2 E_{ref}} \right)^{n/2} \right] \right]^* 2 \alpha f_p E dE \\ &= 2 \alpha f_p \bar{E} \quad mA \int_0^{\infty} E_*^m \exp(-A E_*^m) \left[ 1 - \exp \left[ - \left( \frac{\sigma^2 E_*}{\gamma^2} \right)^{n/2} \right] \right] dE_* \end{aligned}$$

$$= 2 \alpha f_p \bar{E} f_1(\sigma, \gamma, n) \quad [20]$$

The result is that the mean dissipation is the dissipation in waves with the mean energy, times a function of the wave energy relative to the water depth. This function  $f_1$  is less than or equal to 1, and depends on the local wave height to water depth ratio  $\sigma$  and on the empirical coefficients  $\gamma$  and  $n$ .

### Rayleigh distribution

The Rayleigh distribution is a special case of equation [16] for  $m$  equal to 1. It has been used by Thornton and Guza (1983), in combination with a slightly different formulation for the dissipation. The mean dissipation follows immediately from equation [20] and is given by:

$$\begin{aligned} \bar{D} &= 2 \alpha f_p \bar{E} \int_0^{\infty} E_* \exp(-E_*) \left[ 1 - \exp\left[-\left(\frac{\sigma^2}{\gamma^2} E_*\right)^{n/2}\right] \right] dE_* \\ &= 2 \alpha f_p \bar{E} f_2(\sigma, \gamma, n) \end{aligned} \quad [21]$$

### Clipped Rayleigh distribution

The clipped Rayleigh distribution as proposed by Battjes and Janssen (1978) is based on the assumptions that the wave heights are Rayleigh-distributed up to a maximum wave height, that all higher waves are simply cut off to this height, that all waves having this maximum height are breaking and that only these waves are breaking. This can be translated to our concept by letting the value of  $n$  in the probability of breaking go to infinity, in which case the function becomes a step function: zero for  $E/E_{ref} < \gamma^2$ , unity for  $E/E_{ref} \geq \gamma^2$ . The maximum wave energy is defined by:

$$E_m = \gamma^2 E_{ref} \quad [22]$$

Since the probability density function has a 'spike' at  $E=E_m$ , with an area equal to the fraction of breaking waves  $Q_b$ , and since the probability of breaking equals unity at this energy, we get for the mean dissipation:

$$\begin{aligned} \bar{D} &= \int_0^{\infty} p(E) P_b(E) D_b(E) dE = Q_b D_b(E_m) \\ &= Q_b 2 \alpha f_p E_m = 2 \alpha f_p \bar{E} \frac{\gamma^2}{\sigma^2} Q_b \end{aligned} \quad [23]$$

In the clipped Rayleigh distribution, the fraction of breaking waves is defined by the implicit relation:

$$Q_b = \exp \left[ - \frac{1-Q_b}{\bar{E}/E_m} \right] \quad [24]$$

This relation yields a unique function of  $\bar{E}/E_m = \sigma^2/\gamma^2$ , so:

$$\bar{D} = 2 \alpha f_p \bar{E} f_3(\sigma, \gamma) \quad [25]$$

For the three parametric energy distributions, we get similar expressions for the mean dissipation. For given values of the calibration parameters  $\gamma$  and  $n$  the functions  $f_1$ ,  $f_2$  and  $f_3$  depend only on  $\sigma$ . Therefore it is easy to generate tables of these functions and to interpolate from these tables when solving the mean energy balance equation.

#### 4. Calibration of the models

Three datasets, containing a total of 11 tests, were used to calibrate the probabilistic model and the parametric models, viz. those reported in Battjes & Janssen (1978), Stive (1985) and Hotta & Mizuguchi (1980). A summary of the characteristics of the profile and incident wave conditions is given in Table 1. All sets pertain to irregular waves incident perpendicular to a beach. The letter L under 'Type' stands for laboratory test, F stands for field test.

Test	Source	Type	$h_0$ (m)	$H_{E,0}$ (m)	$f_p$ (Hz)
MS10	Stive(1985)	L,plane	0.70	.142	.341
MS40	Stive(1985)	L,plane	0.70	.135	.633
BJ2	Battjes&Janssen (1978)	L,plane	0.70	.144	.511
BJ3	Battjes&Janssen (1978)	L,plane	0.70	.122	.383
BJ4	Battjes&Janssen (1978)	L,plane	0.70	.143	.435
BJ11	Battjes&Janssen (1978)	L,barred	0.70	.137	.450
BJ12	Battjes&Janssen (1978)	L,barred	0.70	.121	.443
BJ13	Battjes&Janssen (1978)	L,barred	0.70	.104	.467
BJ14	Battjes&Janssen (1978)	L,barred	0.70	.118	.481
BJ15	Battjes&Janssen (1978)	L,barred	0.70	.143	.498
HotMiz	Hotta&Mizuguchi (1980)	F,barred	1.65	.527	.113

The parameter for which the calibration was performed is the overall energy-based wave height often (confusingly) referred to as  $H_{rms}$ . Here it will be termed  $H_E$ :

$$H_E = \sqrt{\frac{8\bar{E}}{\rho g}} \quad [26]$$

In deep water,  $H_E$  is equal to the root-mean-square wave height  $H_{rms}$ ; in shallow water, due to non-linearity of the waves, the parameters deviate from each other.

The seawardmost data point, having a wave height  $H_{E,0}$ , is used as a boundary condition for the models. For a given set of calibration points, the energy distribution across each profile is computed and compared to the measured distribution. Two indicators of the overall accuracy of the models are computed, viz. the root-mean-square relative error  $\epsilon_{rms}$  and the relative bias (mean error)  $\epsilon_{mean}$ :

$$\epsilon_{rms} = \sqrt{\frac{1}{N} \sum \left[ \frac{H_{E,comp}}{H_{E,0}} - \frac{H_{E,meas}}{H_{E,0}} \right]^2} / \frac{1}{N} \sum \frac{H_{E,meas}}{H_{E,0}} \quad [27]$$

$$\epsilon_{mean} = \sum \left[ \frac{H_{E,comp}}{H_{E,0}} - \frac{H_{E,meas}}{H_{E,0}} \right] / \sum \frac{H_{E,meas}}{H_{E,0}} \quad [28]$$

As is apparent from the formulae, the errors were scaled with the incident wave height; this is to give data points comparable weights regardless of the scale of the tests or the incident conditions.

From preliminary computations, it turned out that the results were not very sensitive to the value of  $n$ , which indicates the steepness of the curve which describes the probability of breaking. Realistic results were obtained both for  $n=10$  and for  $n=20$ .

The optimum combination of the coefficients  $\alpha$  and  $\gamma$  was obtained by drawing isolines of the error indicators in the  $\alpha, \gamma$  plane, for both values of  $n$ , and visually determining the approximate location of zero mean error and minimum rms error. Plots of these isolines are given in Figures 2a to 2g. By refining the  $\alpha, \gamma$  grid locally and looking at the numerical output, a more accurate location of this optimum was then found.

In all cases the optimum  $\alpha, \gamma$ -combination is found close to the line  $\alpha=1$ . As a constant value of  $\alpha$  facilitates the comparison of the different models, the value of  $\alpha$  was fixed at 1, and optimum  $\gamma$ -values were determined for each model and  $n$ -value. The results are given in Table 2.

Table 2. Optimum $\gamma$ -values and relative rms error for $\alpha=1$ and $n=10, 20$ 11 datasets, 159 points					
Model	$n$	$\alpha$	$\gamma$	$\epsilon_{rms}$	Fig.
Probabilistic	10	1.0	0.55	0.045	2a
	20	1.0	0.53	0.054	2b
Weibull	10	1.0	0.54	0.057	2c
	20	1.0	0.52	0.057	2d
Rayleigh	10	1.0	0.57	0.062	2e
	20	1.0	0.57	0.063	2f
Clipped Rayleigh	-	1.0	0.66	0.056	2g

Apparently, all models can be calibrated to give reasonably accurate predictions of the spatial wave energy variation for a fixed combination of calibration coefficients. The probabilistic model seems the most accurate, whereas the parametric Rayleigh model with  $n$  set at 10 or 20 gives the greatest error.

The clipped Rayleigh model ( $n = \infty$ ) seems to do well with a constant  $\alpha, \gamma$ -combination. Battjes and Stive (1985) used an expression for the maximum wave height which includes the effect of wave steepness; consequently they found that the calibration coefficient  $\gamma$  showed a dependence of the deep water steepness. It seems that using the simpler relation [22] removes this dependence. The optimum  $\gamma$ -values for the Weibull parametric model and the probabilistic model agree closely, which indicates that the energy distributions resulting from the probabilistic model are similar to the shape assumed beforehand in the parametric model.

In the Rayleigh model with finite  $n$ , higher wave energy is possible than in the Weibull model, so the probability of breaking for a given energy must decrease in order to get the same mean dissipation. This results in a higher optimum value of  $\gamma$ .

In the clipped Rayleigh model, it is assumed that all breaking waves have the maximum wave energy. The  $\gamma$ -value in this case indicates the level where most dissipation takes place. The optimum value of 0.66 is not in contradiction with the other models.

A value of  $n$  equal to 10 gives slightly better results than  $n$  equal to 20; for the probabilistic model a value of 5 was tried but produced no better results. The value of  $n$  was kept at 10 in all further computations.

In Figures 3a through 3i, the wave height profiles as computed with the probabilistic model, for  $n$  equal 10, are compared with the measured wave height profiles, for all calibration tests. The agreement is quite good, especially considering that all computations were performed with the same set of coefficients.

## 5. Verification

The primary goal of this study is to formulate the time-varying dissipation as a function of local wave parameters. As this is only one of the internal parameters in the models described above, the fact that the mean wave energy (the external parameter) is predicted accurately is not sufficient; errors in internal parameters may be cancelled out by each other.

The dependence scheme in Figure 4. indicates which other internal parameters must be checked in order to gain confidence in the formulation of the expected value of the slowly-varying dissipation.

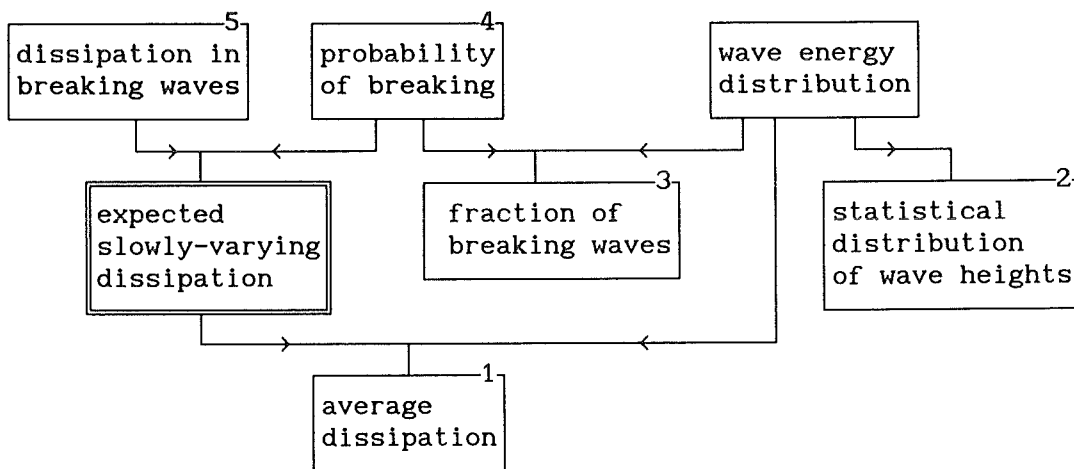


Figure 4. Dependence scheme dissipation model

In the following Sections, the numbered items in the dependence scheme will be discussed separately; afterwards, conclusions are drawn on the accuracy of the model of the expected slowly-varying dissipation.

### 5.1 Average dissipation

As has been shown in the previous Section, the average dissipation is modelled accurately. An independent verification is given by two additional datasets, viz. those reported by Ebersole and Hughes (1987) and by Van der Meer (1990). The incident wave conditions are given in Table 3.

Table 3. Experimental parameters verification sets					
Test	Source	Type	$h_o$ (m)	$H_{E,o}$ (m)	$f_p$ (Hz)
D41400	Ebersole&Hughes (1987)	F,barred	1.75	.600	.089
D41510	Ebersole&Hughes (1987)	F,barred	1.49	.706	.089
D50955	Ebersole&Hughes (1987)	F,barred	2.14	.431	.088
D51055	Ebersole&Hughes (1987)	F,barred	1.80	.353	.089
D51352	Ebersole&Hughes (1987)	F,barred	2.19	.452	.092
D51525	Ebersole&Hughes (1987)	F,barred	1.94	.374	.090
D60915	Ebersole&Hughes (1987)	F,barred	1.40	.360	.078
D61015	Ebersole&Hughes (1987)	F,barred	2.14	.296	.076
D61300	Ebersole&Hughes (1987)	F,barred	2.43	.346	.099
T007	van der Meer (1990)	L,step	0.56	.049	.403
T015	van der Meer (1990)	L,step	0.56	.071	.438
T110	van der Meer (1990)	L,step	0.56	.099	.513
T12	van der Meer (1990)	L,step	0.71	.059	.488
T13	van der Meer (1990)	L,step	0.66	.109	.488
T212	van der Meer (1990)	L,step	0.61	.072	.645
T216	van der Meer (1990)	L,step	0.61	.068	.403
T322	van der Meer (1990)	L,step	0.66	.121	.513

The dataset by Ebersole and Hughes was obtained in the field during the DUCK85 campaign. It concerns long-period swell incident perpendicular to an almost prismatic beach. The measurements were carried out with the photopole technique (Hotta and Mizuguchi, 1980). The measurements have been studied in detail by Dally (1990). A problem with hindcasting these experiments with the present model is that the wave height distributions at the outermost measuring point deviate significantly from either Rayleigh or Weibull distributions; therefore we cannot expect very good agreement. Still, the measurements have been included as a severe test case. The models were applied with their pre-calibrated coefficient values:  $\alpha=1$ ,  $n=10$  and  $\gamma$  as in Table 2. Model performance was reasonable for all models: for the 9 experiments, the mean error was less than 2% for all models and the rms error was in the order of 13%. The probabilistic model was not significantly better than the parametric models.

The dataset by Van der Meer concerns laboratory cases of waves incident on a profile with a steep step followed by a very gently sloping bottom. Here, the parametric models show a mean error in the order of 1% and a rms error in the order of 11% over a total of 8 tests. The probabilistic model shows a mean error of almost 5%, but a lower rms error of 8%. The general shape of the energy distributions over the profile is represented best by the probabilistic model; hence the lower rms error.

The error indicators were also computed over all tests considered in this study; the results are given in Table 4.

Table 4. Relative mean and rms error 28 tests, 389 points					
Model	n	$\alpha$	$\gamma$	$\epsilon_{\text{mean}}$	$\epsilon_{\text{rms}}$
Probabilistic	10	1.0	0.55	0.013	0.088
Weibull	10	1.0	0.54	0.000	0.099
Rayleigh	10	1.0	0.57	0.011	0.099
Clipped Rayleigh	$\infty$	1.0	0.66	0.000	0.096

All models can be used to predict the variation of the mean wave energy over the profile; the probabilistic model is slightly more accurate in this respect. A comparison between the measured wave height profiles and those computed with the probabilistic model is given in Figures 3a to 3z.

## 5.2 Statistical distribution of wave heights

At present, no data are available on the probability distribution of the wave energy; data on wave height probability distributions are available. With the help of non-linear theory, wave heights can be estimated from wave energy levels. If the variation of statistical wave height parameters over the profile is predicted correctly, the underlying energy probability distributions are likely to be correct as well.

The statistical wave height parameters are deduced from the predicted wave energy probability distribution by the following method. The distribution of the linear estimate of the wave height,  $H_l$ , was derived from the wave energy distribution, where  $H_l = \sqrt{8E/\rho g}$ . The statistical parameters  $H_{l,rms}$ ,  $H_{l,1\%}$  and  $H_{l,1\%}$  were computed from this distribution, using the usual definitions. The matching non-linear crest-to-trough heights were then computed with the help of Rienecker & Fenton's (1981) stream function method.

The dataset used is from Stive (1985), tests MS10 and MS40. In Figures 5a and 5b, the distributions of the rms wave height  $H_{rms}$ , the significant wave height  $H_{sig}$  and the wave height exceeded 1% of the time, H1%, as measured and as computed, are given. Qualitatively, the agreement is quite good; quantitatively, the values of H1% are underestimated within the surf zone. This may be due to the presence of long waves; the higher waves are limited in

the model by the mean depth, whereas in reality they are limited by the slowly-fluctuating depth. Also within the surf zone, as can be expected, the values of the rms wave height are overpredicted by non-linear theory, due to the decoupling of the higher harmonics. Still, the wave height distributions are predicted well enough to lend some confidence to the computed energy distributions. Further study is required to confirm this.

### **5.3 Fraction of breaking waves**

The fraction of breaking waves,  $Q_b$ , is the integral of the product of the energy distribution and the probability of breaking at a given energy. Therefore, if the energy distribution is modelled correctly, the fraction of breaking waves can only be correct if the probability of breaking is correct too. In the same two tests from Stive (1985), the fraction of breaking waves was counted visually; measured and predicted values are shown in Figures 5a and 5b. For test MS10, the agreement is quite good, although well inside the surf zone  $Q$  is somewhat underpredicted, by up to 30%. For test MS40, the underprediction is much more serious: up to a factor 3. This seems strange since the dissipation is modelled so well.

A possible explanation is that the peak period during this test was twice as short as during test MS10. The waves therefore tended to be spilling, whereas the bore model only really applies to fully breaking waves with a roller over the whole wave front. In such a case, the criterion that a breaking wave is 'a wave with foam on it' will overestimate the fraction of bore-like breaking waves.

The question is, whether this analysis should lead to an adjustment of the definition of 'breaking wave' or to an adjustment of the model of the dissipation in a breaking wave. This should be resolved in further study; for now, the computed fraction of breaking waves should be interpreted as the fraction of fully-breaking, bore-like waves.

### **5.4 Probability of breaking**

The probability of breaking as a function of wave height has been investigated by some authors (Thornton and Guza, 1983; Dally, 1990). This gives a qualitative check on the shape of this probability as a function of energy. However, the available data do not enable a direct plot of the probability of breaking against the wave energy, for given water depths, so a direct quantitative check cannot be made. As is also apparent from the previous Section, further study is required on this aspect of the model.

## 5.5 Dissipation in breaking waves

An interesting verification of the formulation of the dissipation in breaking waves is obtained from the measurements of Stive (1984), for regular waves. On page 109 of his paper, he presents graphs of a non-dimensional dissipation  $A_\epsilon$ , defined as the ratio of the dissipation rate derived from measured energy flux gradients and the dissipation according to a hydraulic jump:

$$D_b = A_\epsilon \frac{1}{4} \rho g f H^3 \frac{h}{d_1 d_2} \quad [29]$$

where  $d_1$  is the depth in front of the breaker and  $d_2$  is the depth at the crest. The values of  $A_\epsilon$  are in the range of 1.5 to 2.5. If we now assume:

$$\frac{H h}{d_1 d_2} = \gamma_3 \quad [30]$$

we get a similar expression to our equation [4] if  $\alpha = A_\epsilon \gamma_3$ . With the order of magnitude estimates  $H/h \approx 0.5$ ,  $d_1/h \approx 0.8$  and  $d_2/h \approx 1.3$ ,  $\gamma_3$  is in the order of 0.5, which leads to an  $\alpha$ -value in the order of 1. This is in agreement with the optimum value found in the calibration.

## 5.6. Conclusions on verification

From the verification presented here we may draw the conclusion that the mean dissipation is modelled correctly and that there are indications that the wave energy distribution is also modelled correctly; therefore, the expected time-varying dissipation must be reasonably accurate. This term is again composed of two terms, viz. the time-varying dissipation in breaking waves and the probability of breaking. There is an indication that the first of these terms is modelled correctly; on the probability of breaking there is still some uncertainty. Qualitatively, there is agreement between measured and predicted fractions of breaking waves; quantitatively, they are somewhat underpredicted, although of the right order of magnitude.

## 6. Conclusions

The existing parametric model according to Battjes and Janssen has been improved in the sense that the internal parameters are more realistic; also, the dependence of the calibration coefficients on wave steepness has vanished. A parametric model based on a Weibull distribution has been added to this class of models, for which the distributions closely resemble those resulting from the probabilistic model. All three parametric models can be used to

predict with reasonable accuracy the spatial distribution of the mean wave energy; the one based on a Weibull distribution is the most accurate, and the model based on the Rayleigh distribution the least accurate.

The probabilistic model presented has been shown to follow from the wave action equation if the group velocity is assumed to be constant in time and effects of surfbeat can be neglected. These restrictions are less severe than those for the earlier models in this class, which require a negligible variation of the propagation velocity of individual waves. One set of equations is used throughout the shoaling and breaking region, as opposed to earlier models in this class. The model can be used to predict the transformation of the probability distribution of the wave energy through the surf zone. With the help of a non-linear wave theory, wave height characteristics can be derived from the energy distributions.

The calibrated and verified equation [7] for the expected time-varying dissipation can be readily used in wave propagation models that take into account variations on the time-scale of wave groups.

#### **Acknowledgements**

This work was undertaken as part of the MAST G6 Coastal Morphodynamics research programme. It was funded jointly by the Coastal Genesis programme of The Netherlands' Rijkswaterstaat and by the Commission of the European Communities, Directorate General for Science, Research and Development, under MAST contract no. 0035. The author would like to thank his colleague M.J.F. Stive and Prof. J.A. Battjes for their constructive remarks on a draft version of this paper.

#### **References**

- Battjes, J.A. and J.P.F.M. Janssen ( 1978 )  
Energy loss and set-up due to breaking of random waves  
Proc. 16th Int. Conf. Coastal Engineering, pp 569-587, ASCE, New York, 1978
- Battjes, J.A. and M.J.F. Stive ( 1985 )  
Calibration and verification of a dissipation model for random breaking waves  
Journal of Geophysical Research, vol. 90, No. C5, pp. 9159-9167, 1985
- Dally, W.R. ( 1990 )  
Random breaking waves: Field verification of a wave-by-wave algorithm for engineering application  
*in press*
- Dally, W.R., R.G. Dean and R.A. Dalrymple ( 1984 )  
A model for breaker decay on beaches  
Proc. 19th Int. Conf. Coastal Engineering, pp. 82-98, ASCE, New York, 1984

- Ebersole, B.A. and S.A. Hughes ( 1987 )  
 Duck85 photopole experiment  
 U.S. Army Waterways experiment station, misc. paper CERC-87-18, Vicksburg,  
 1987
- Glukhovskiy, B.Kh. ( 1966 )  
 Issledovaniye morskogo vetrovogo volneniya (investigation of sea wind waves)  
 Gidrometeoizdat, Leningrad, 1966
- Hotta, S. and M. Mizuguchi ( 1980 )  
 A field study of waves in the surf zone  
 Coastal Engineering in Japan, vol. XXIII, Japan Soc. of Civil Engineers, Tokyo
- Klopman, G. and M.J.F. Stive ( 1989 )  
 Extreme waves and wave loading in shallow water  
 Paper presented at E&P Forum Workshop "Wave and current kinematics and  
 loading", Paris, France, 25-26 Oct. 1989
- LeMehaute, B. ( 1962 )  
 On non-saturated breakers and the wave run-up  
 Proc. 8th Int. Conf. Coastal Engineering, pp 1178-1191, ASCE, New York, 1962
- List, J.H. ( 1990 )  
 A model for two-dimensional surf beat  
 subm. Journal of Geophysical Research, 1990
- Mase, H. and Y. Iwagaki ( 1982 )  
 Wave height distributions and wave grouping in surf zone  
 Proc. 18th Int. Conf. Coastal Engineering, pp. 58-76, ASCE, New York, 1982
- Mizuguchi, M. ( 1982 )  
 Individual wave analysis of irregular wave deformation in the nearshore zone  
 Proc. 18th Int. Conf. Coastal Engineering, pp. 485-504, ASCE, New York, 1982
- Rienecker, M.M. and J.D. Fenton ( 1981 )  
 A Fourier approximation method for steady water waves  
 J. Fluid Mech. (1981), vol 104, pp. 119-137
- Roelvink, J.A. ( 1991 )  
 Modelling of cross-shore flow and morphology  
 Proc. ASCE Specialty Conf. 'Coastal Sediments', Seattle, 1991, pp 603-617
- Sato, S. and N. Mitsunobu (1991)  
 A numerical model of beach profile change due to random waves  
 Proc. ASCE Specialty Conf. 'Coastal Sediments', Seattle, 1991, pp 674-687
- Schaeffer, H.A. and I.G. Jonsson ( 1990 )  
 Theory versus experiments in two-dimensional surf beats  
 Proc. 22nd Int. Conf. Coastal Engineering, Delft, 1990, pp 1131-1143
- Stive, M.J.F. ( 1984 )  
 Energy dissipation in waves breaking on gentle slopes  
 Coastal Engineering 8(1984) pp 99-127
- Stive, M.J.F. ( 1985 )  
 A scale comparison of waves breaking on a beach  
 Coastal Engineering 9(1985) pp 151-158
- Stive, M.J.F. and M.W. Dingemans ( 1984 )  
 Calibration and verification of a one-dimensional wave energy decay model  
 Delft Hydraulics Laboratory, report on investigation M 1882, Delft, 1984

Symonds, G. and K.P. Black ( 1991 )  
Numerical simulation of infragravity response in the nearshore  
Proc. 10th Australasian Coastal and Ocean Eng. Conf., Auckland, New Zealand,  
Dec. 1991, pp 339-344.

Symonds, G. and A.J. Bowen ( 1984 )  
Interactions of nearshore bars with incoming wave groups  
Journal of Geophysical Research, vol. 89, no. C2, pp 1953-1959, 1984

Symonds, G., D.A. Huntley and A.J. Bowen ( 1982 )  
Two-dimensional surf beat: long wave generation by a time-varying breakpoint  
Journal of Geophysical Research, vol. 87, no.C1, pp 492-498, 1982

Thornton, E.B. and R.T. Guza ( 1983 )  
Transformation of wave height distribution  
Journal of Geophysical Research, vol. 88, pp. 5925-5938, 1983

### List of Figures

1. Plot of the function  $Y = 1 - \exp(-X^{n/2})$  for  $n = 5, 10, 20$
- 2.a-g Isolines of rms-error (drawn lines) and mean error (interrupted lines) for all points in calibration sets.
- 3.a-z Comparison of measured and computed spatial distribution of  $H_E$ , calibration sets and verification sets
4. Dependence scheme dissipation model
- 5.a-b Measured vs. computed values of  $H_E$ ,  $H_{rms}$ ,  $H_{sig}$ ,  $H_{1\%}$  and  $Q$ ; tests from Stive (1985).

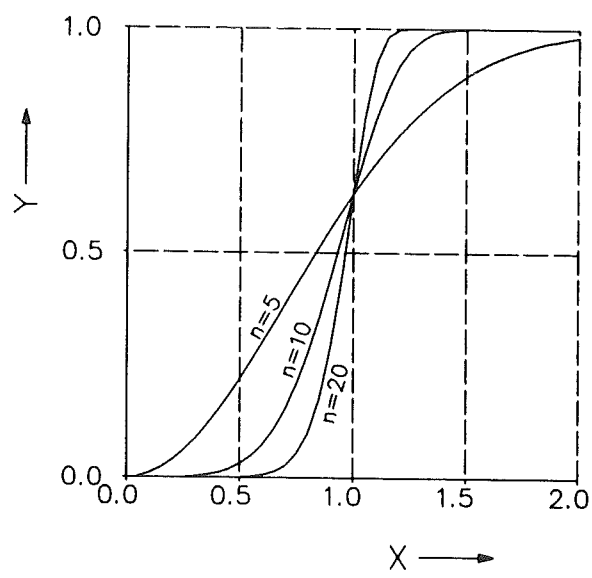


FIG. 1

Probabilistic model  
n=10

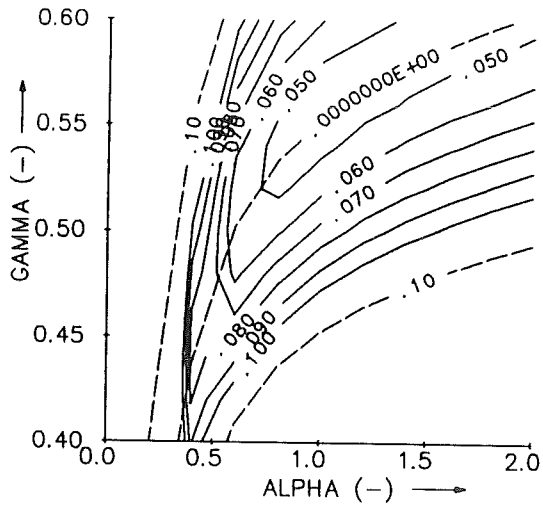


Fig. 2a

Probabilistic model  
n=20

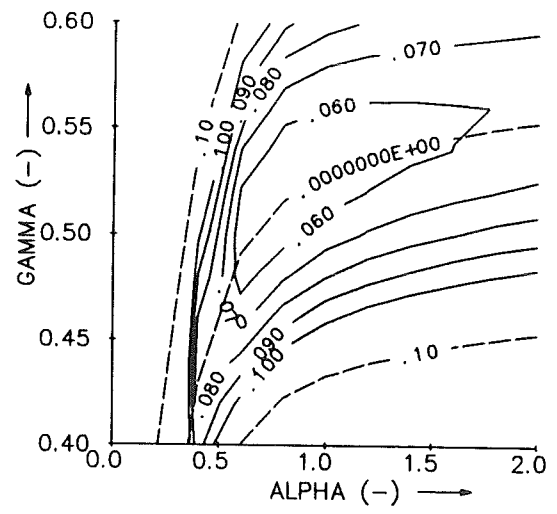


Fig. 2b

WEIBULL  
n=10

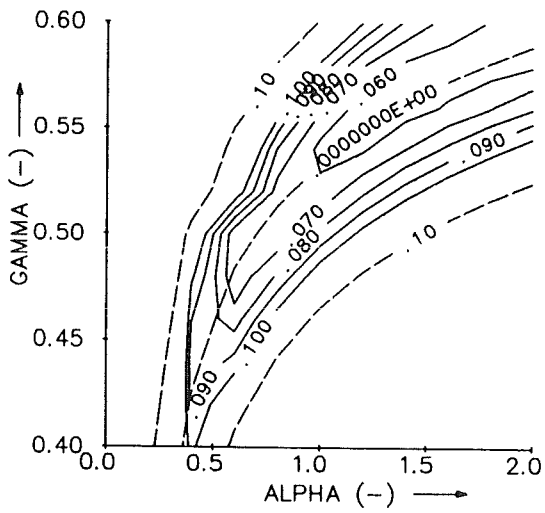


Fig. 2c

WEIBULL  
n=20

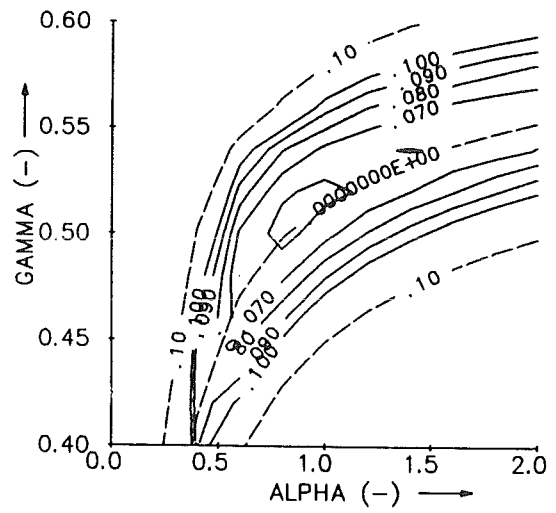


Fig. 2d

Rayleigh  
 $n=10$

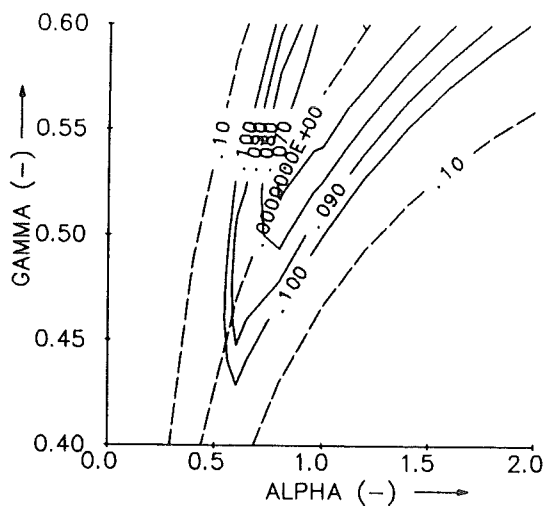


Fig. 2e

Rayleigh  
 $n=20$

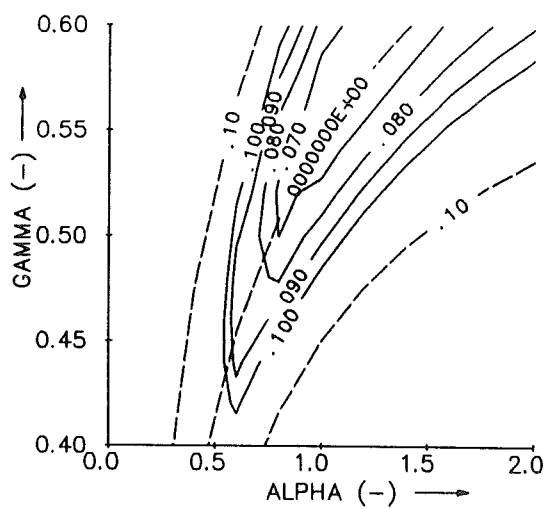


Fig. 2f

Clipped Rayleigh

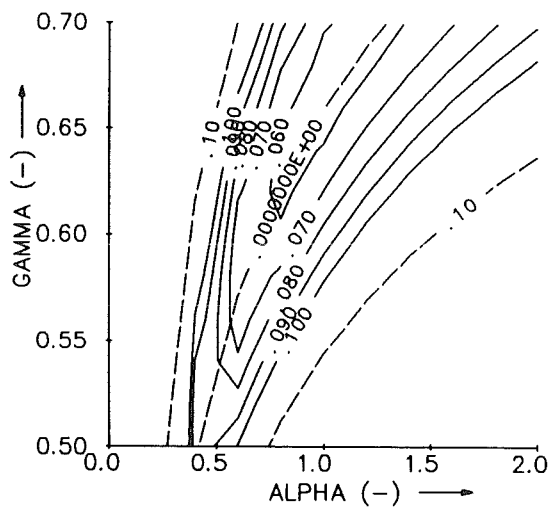


Fig. 2g

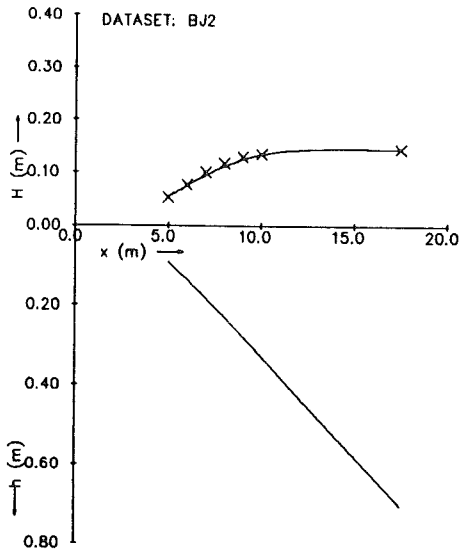


Fig. 3a

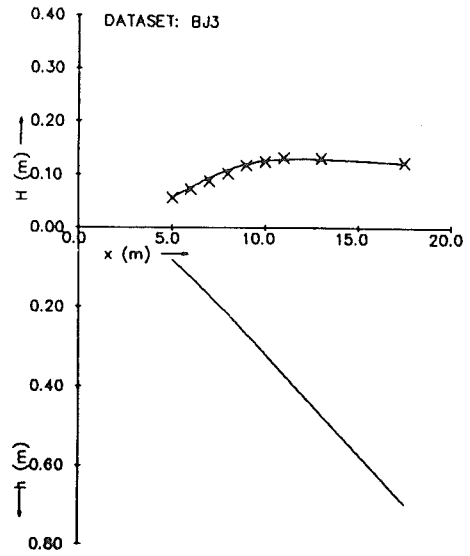


Fig. 3b

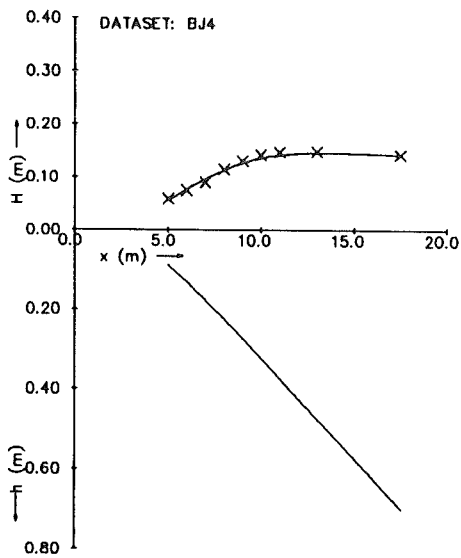


Fig. 3c

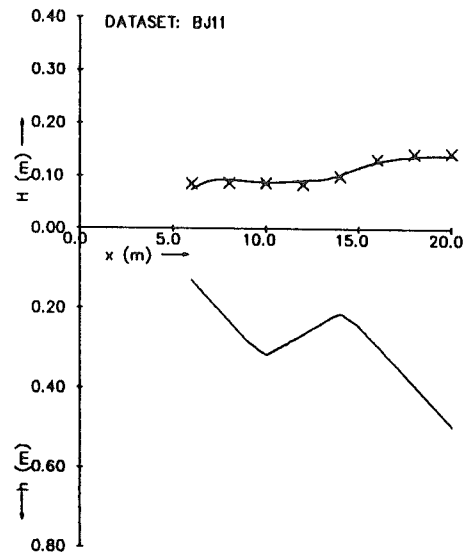


Fig. 3d

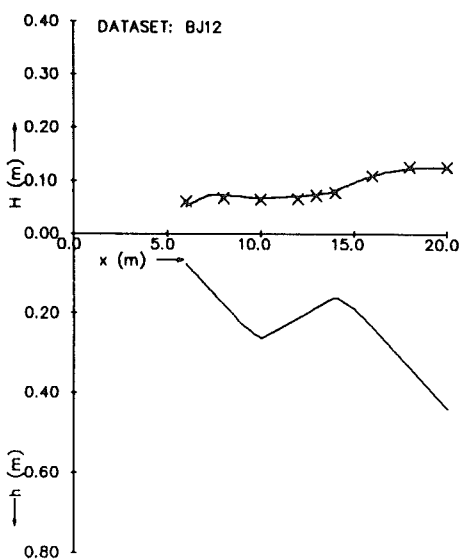


Fig. 3e

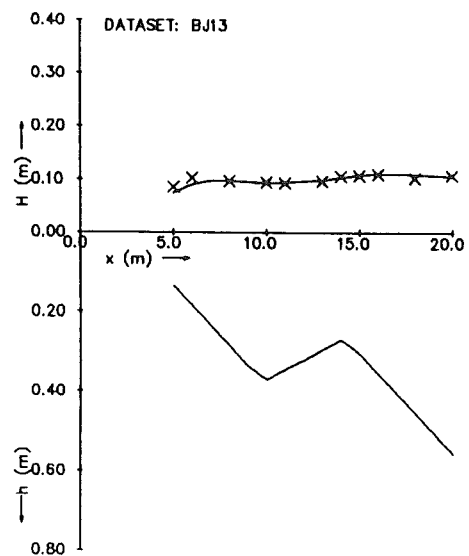


Fig. 3f

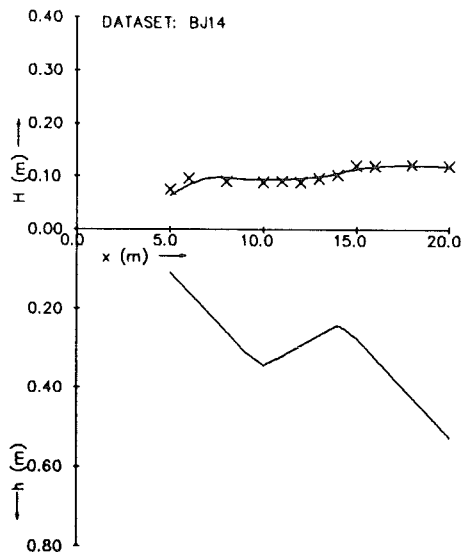


Fig. 3g

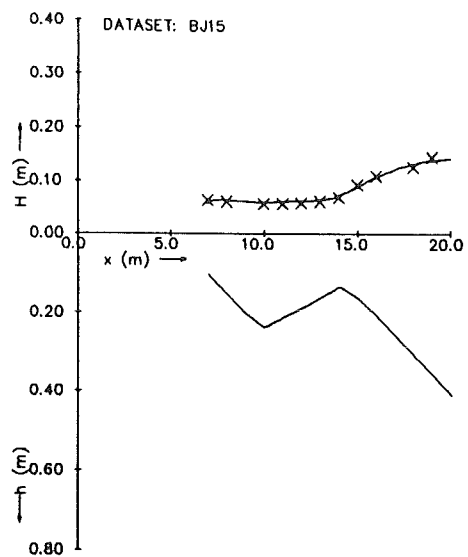


Fig. 3h

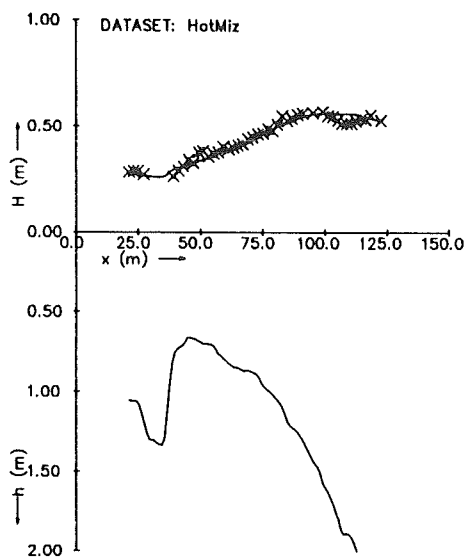


Fig. 3i

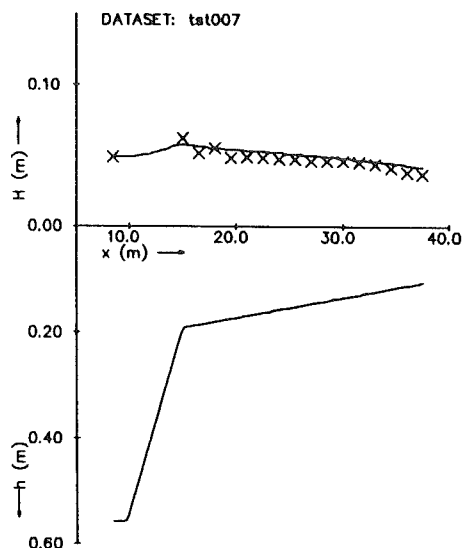


Fig. 3j

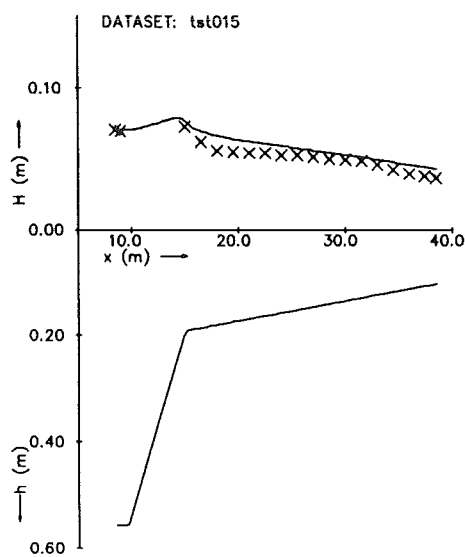


Fig. 3k

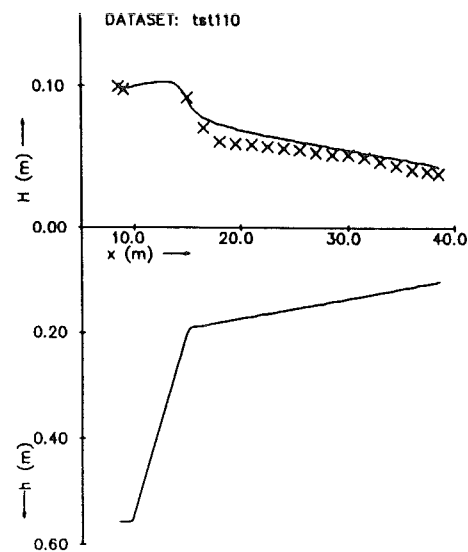


Fig. 3l

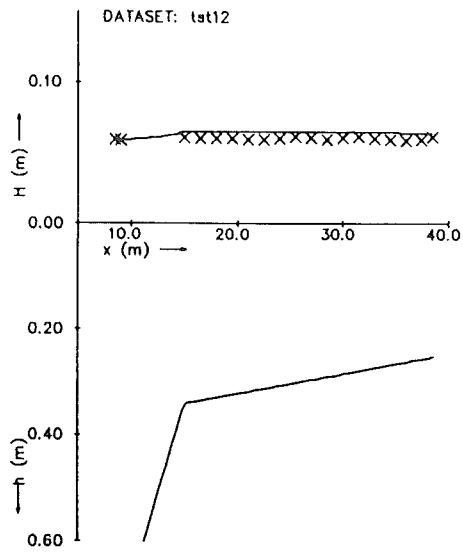


Fig. 3m

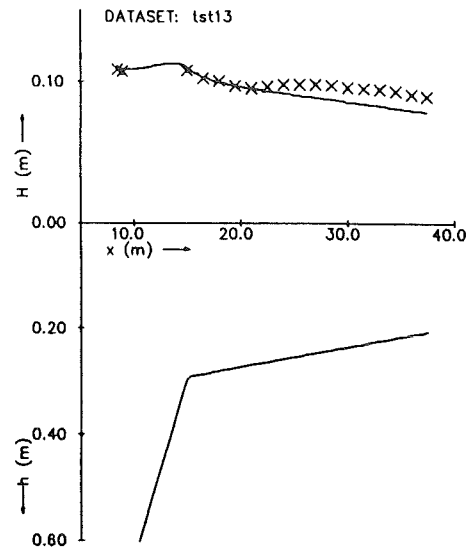


Fig. 3n

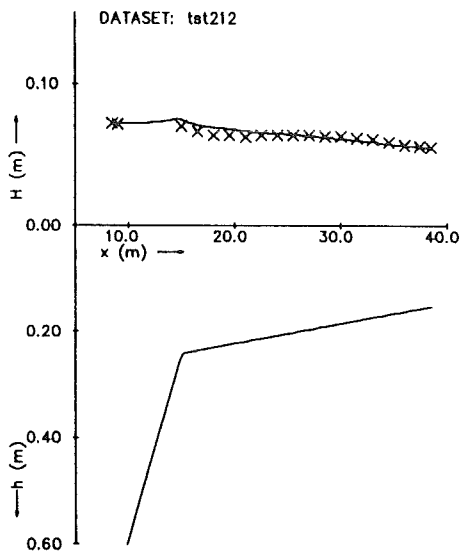


Fig. 3o

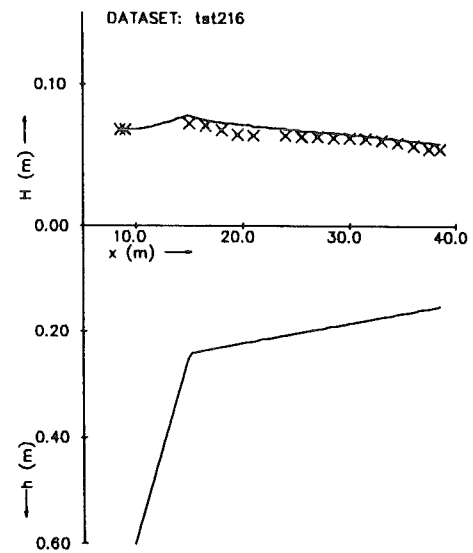


Fig. 3p

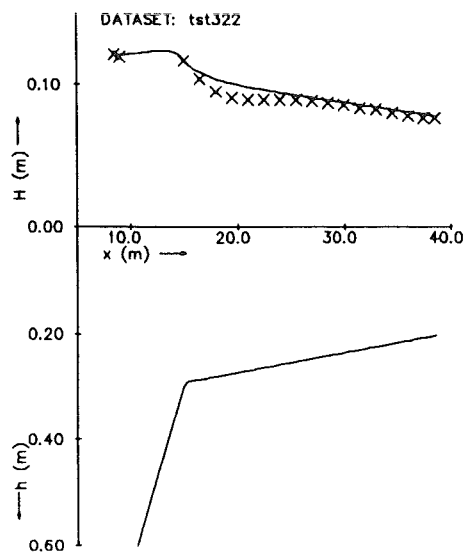


Fig. 3q

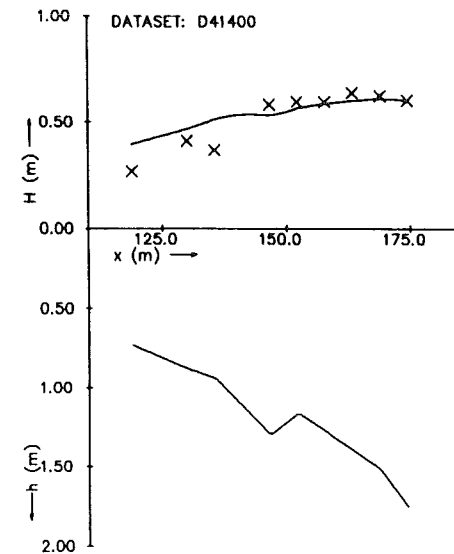


Fig. 3r

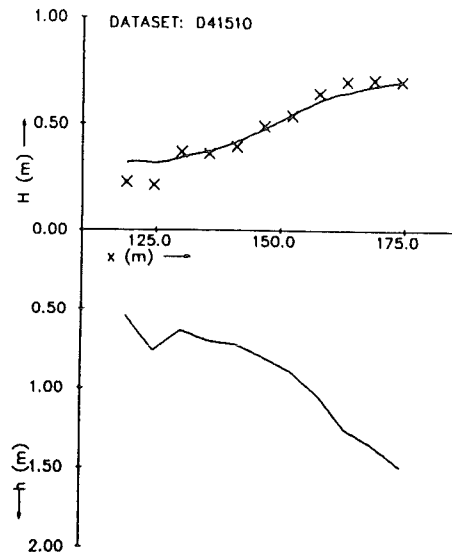


Fig. 3s

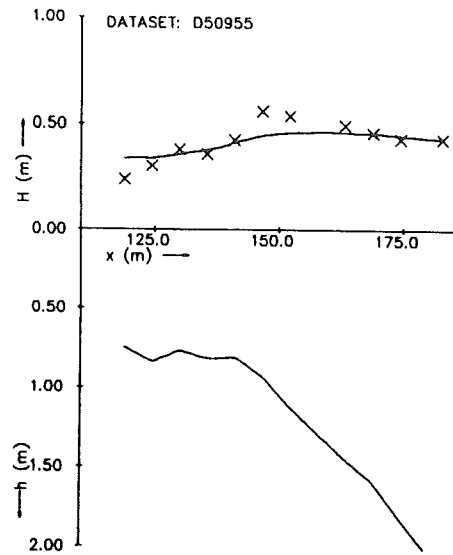


Fig. 3t

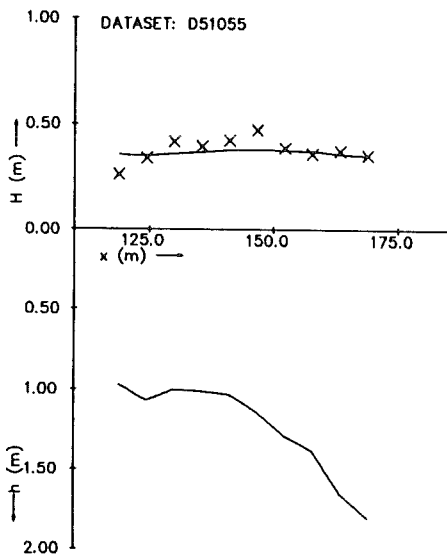


Fig. 3u

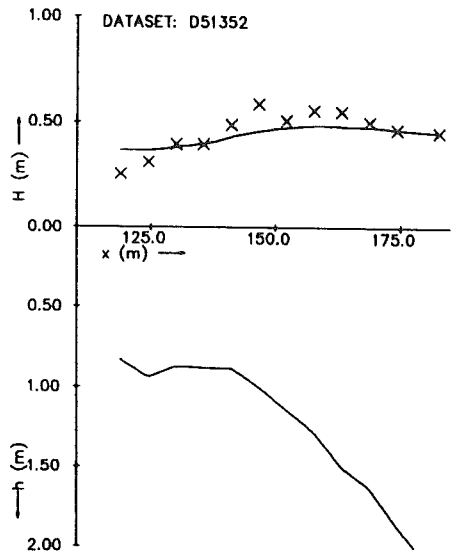


Fig. 3v

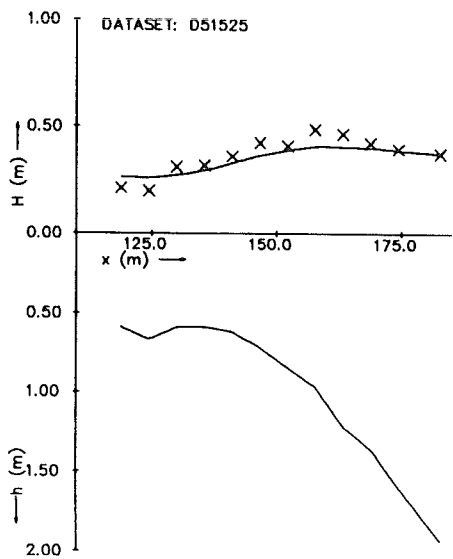


Fig. 3w

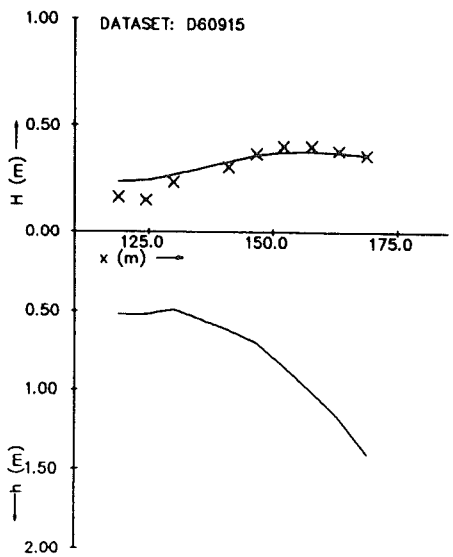
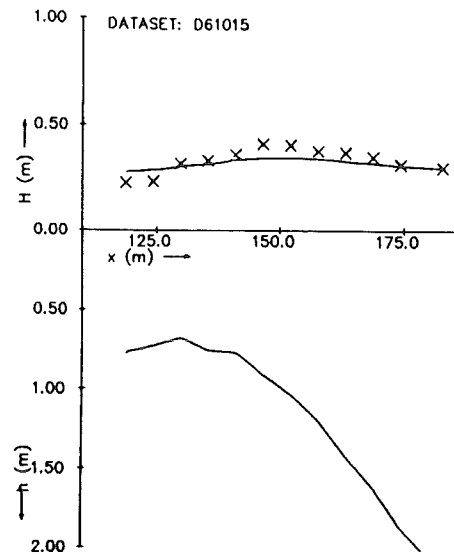
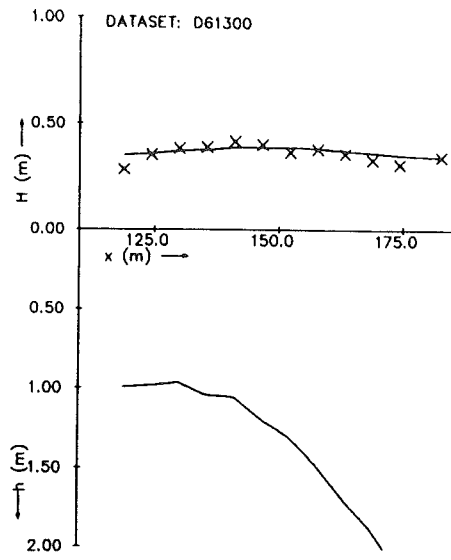


Fig. 3x



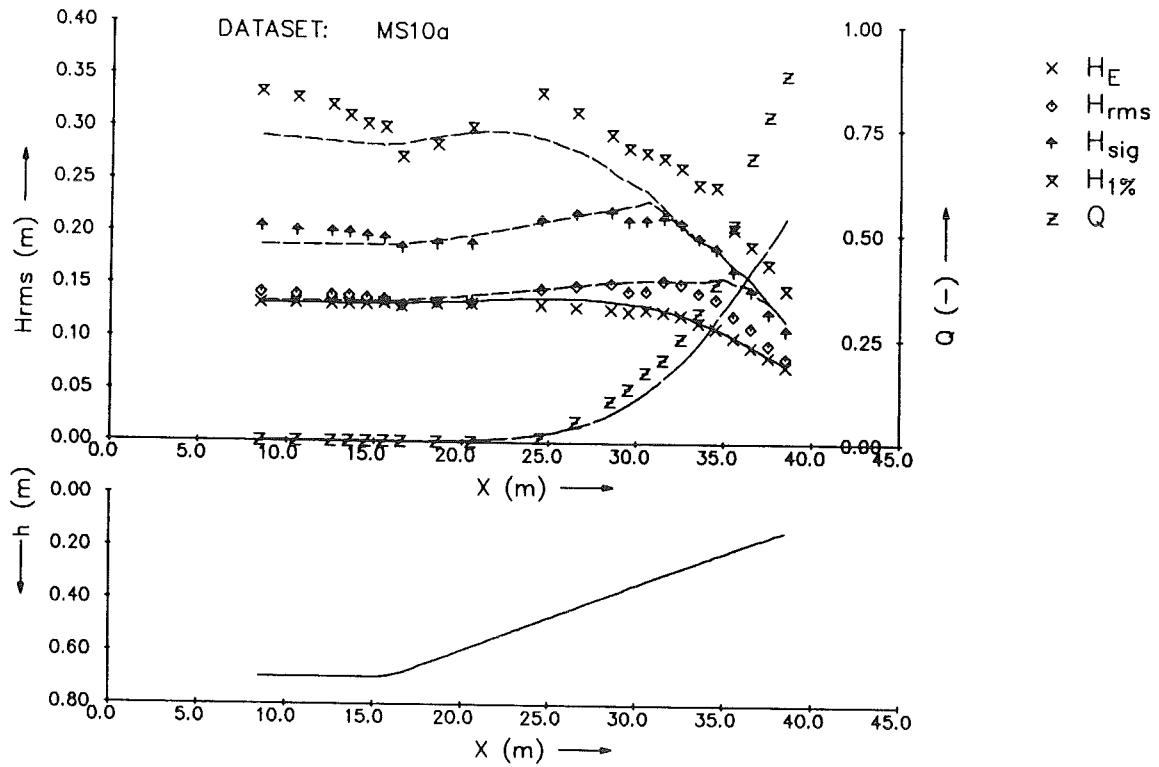


Fig. 5a

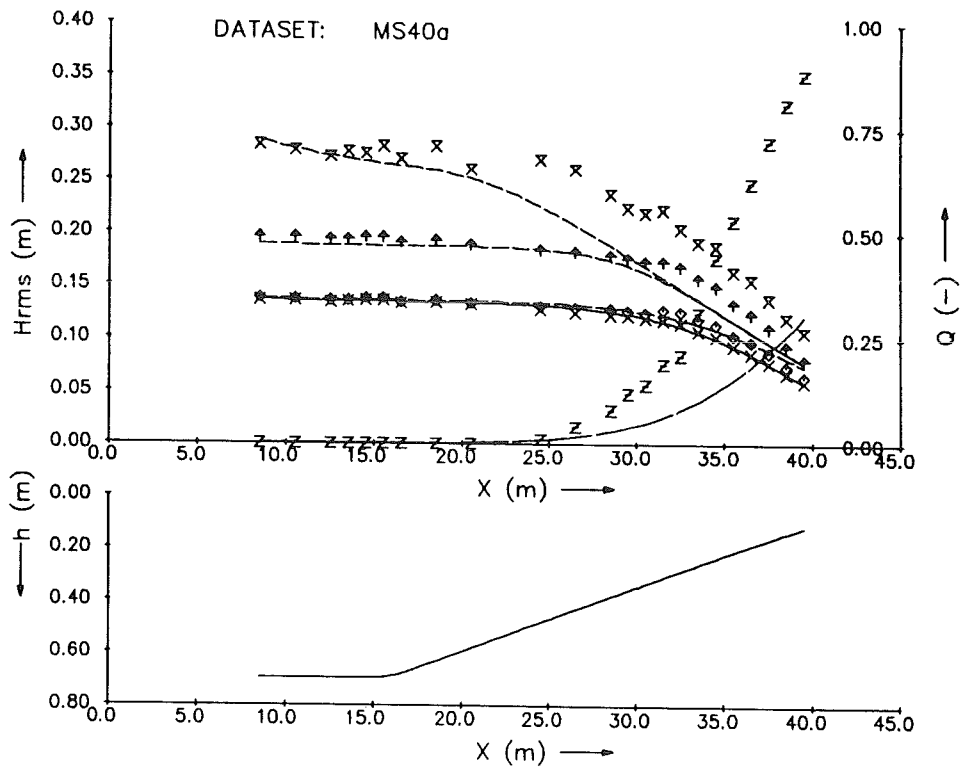


Fig. 5b